Grain size modulation on BaTiO$_3$ nanoparticles synthesized at room temperature

Jian Quan Qi [a,b,*], Li Sun [b], Xi Wei Qi [a], Yu Wang [b], Helen Lai Wah Chan [b]

[a] Department of Materials Sciences & Engineering, Northeastern University at Qinhuangdao Branch, Qinhuangdao, Hebei 066004, PR China
[b] Department of Applied Physics and Materials Research Center, The Hong Kong Polytechnic University, Hong Kong, PR China

ARTICLE INFO

ABSTRACT

A new method is developed to synthesize massive BaTiO$_3$ nanoparticles directly at room temperature. With this method, the synthesis efficiency is improved and mass preparation can be realized. Also, the grain size of the as-prepared nanoparticles can be modulated from several nanometers to 40 nm through proper selection of the content of water and the alkanol chain length of the dispersant. It was found that smaller water content and a larger alkanol chain length of the dispersant will lead to a finer grain size. The mechanisms of the grain size modulation of BaTiO$_3$ nanoparticles are also discussed.

© 2011 Elsevier Inc. All rights reserved.

1. Introduction

With high ferroelectric properties, Barium titanate (BaTiO$_3$) based materials are widely used in electronic industry [1]. Two important applications include multilayer ceramic capacitors (MLCCs) [2] and positive temperature coefficient resistors (PTCRs) [3]. Of all the applications, grain size modulation is very important due to its confinement on the layer thickness of MLCCs and its influence on ceramic sintering activity and doping behaviors, both of which affect the properties of final products. Although many novel synthesis techniques have been developed for such an important material, purposeful modulation on grain size is still a challenge and its mechanisms are not very clear.

To prepare the BaTiO$_3$ based nanostructures, solution chemical routes [4–6] and thermal decomposition of a metal-organic precursor [7–9] were developed, however, an elevated temperatures (typically 100–280 °C) and/or relatively high pressures were often involved in these methods, especially in the hydrothermal method. To decrease the synthesis temperature and obtain finer particles with less agglomeration, much work was done. It has been reported that BaTiO$_3$ nanoparticles could be obtained at relative low temperature by using ethanol–water mixture as solvent [10,11]. Direct synthesis from solution (DSS) was

developed to prepare perovskite nanoparticles with the particle size of 20–70 nm, which was operated at 50–100 °C and normal pressure conveniently by dripping titanium [10] or zirconium [12] alcoxide solution into strong alkaline (i.e. barium hydroxide) solution. Recently, BaTiO$_3$ nanoparticles have been synthesized at room temperature with a biosynthesis method [13,14]. However, this method is costly and uncontrollable, which hinders its application in mass production. There have been some efforts to scale up the preparation of BaTiO$_3$ nanoparticles [15,16]. According to existing methods to prepare BaTiO$_3$ nanoparticles, a much finer grain size is still difficult to obtain and the production efficiency in industry is often limited.

In our study, a simplified method using the standard ceramic process is introduced to synthesize barium titanate nanoparticles in large scale at room temperature [17]. The grain size of the as-prepared nanoparticles can be modulated purposefully and the synthesis efficiency is improved greatly.

2. Experimental procedure

The method was derived from DSS and is carried out in an enclosed system. The spontaneous reaction of alkali to environmental CO$_2$ is avoided and the content of barium carbonate is suppressed in the final products. The reagents Ba(OH)$_2 \cdot$ 8H$_2$O or anhydrous Ba(OH)$_2$ and tetrabutyl titanate[Ti(OC$_4$H$_9$)$_4$] are adopted as starting raw materials to prepare BaTiO$_3$ nanoparticles. Butanol and ethanol are used as a dispersant to compare the effects of alkanol chain length on the grain size of final products.

* Corresponding author at: Department of Materials Sciences & Engineering, Northeastern University at Qinhuangdao Branch, Qinhuangdao, Hebei 066004, PR China. Fax: +86 0335 8051795.
E-mail address: jianquanqi@mail.tsinghua.edu.cn (J.Q. Qi).

The titanium solution is obtained by dissolving 34.0 g of $Ti(OC_4H_9)_4$ in 50.0 ml dispersant. The alkali slurry is prepared by ball milling 31.6 g of $Ba(OH)_2 \cdot 8H_2O$ or 17.1 g $Ba(OH)_2$ with different contents of water in 100.0 ml dispersant for 4 h. The cubage of the milling jar is 250.0 ml. The titanium solution is added into the alkali slurry in the jar and resealed for another 18 h milling at the rate of 200 rpm, after that, homogenous white slurry is obtained. The white slurry is air-dried and $BaTiO_3$ nanoparticles are synthesized. All of the procedures are operated at room temperature. The nanoparticle samples are named as A, B, C and D according to the different dispersant and raw materials as listed in Table 1.

The samples are characterized by X-ray diffraction (XRD) at room temperature on a Philips Diffractometer (Model: X'Pert-Pro MPD) using Cu $K\alpha$ radiation ($\lambda = 0.15406$ nm). The microstructures of powders are observed by scanning electron microscopy (SEM) on a JEOL field-emission SEM (Model: JSM 6335F NT) and transmission electron microscopy (TEM) on a JEOL TEM (Model: JSM2010).

3. Results and discussion

A large quantity (23.0 g) of barium titanate nanoparticles are directly synthesized at room temperature. Fig. 1 shows the XRD profile of the as-prepared nanoparticles synthesized with different dispersants and/or different raw materials. All the samples

Table 1
Synthesis conditions of each samples.

Samples	Dispersant	Raw materials of alkali slurry
A	Absolute ethanol	50.0 gH_2O + 31.6 g $Ba(OH)_2 \cdot 8H_2O$
B	Absolute ethanol	31.6 g $Ba(OH)_2 \cdot 8H_2O$
C	Absolute ethanol	3.6 g H_2O + 17.1 g $Ba(OH)_2$
D	Butanol	3.6 g H_2O + 17.1 g $Ba(OH)_2$

have a perfectly crystallized perovskite structure. As ball milling is used as a means of mechanical mixing, the quantity of barium hydroxide is not limited by its solubility in the solvent during the synthesis process, and thus the synthesis efficiency is improved greatly. For example, a large quantity of solvents has to be used in conventional solution method, since the solubility of barium hydroxide is small (i.e. 20 °C 3.9 g/100 ml water). In our method, only a small quantity of dispersant is needed and the batch of product can be easily enlarged.

There is a slight dose of $BaCO_3$ in samples A and B indexed as 3.3% and 5.0%, respectively, using an external reference method [18]. As our synthesis is in an enclosed system, one possible source of carbonate is the raw material, $Ba(OH)_2 \cdot 8H_2O$, which may react with CO_2 in air during its storage. On the other hand, the carbonates are not found in the profiles of samples C and D because their raw material $Ba(OH)_2$ is sealed and airproof during storage. All the peaks of the XRD profiles have a line broadening effect in our samples and this effect is remarkable in samples C and D. Such a line broadening effect is caused by the fine grains, and the grain size can be estimated using Scherrer's equation:

$$L = \frac{K\lambda}{\beta \cos\theta} \qquad (1)$$

where L is the crystallite size, λ the wavelength of the X-ray radiation (0.15418 nm for Cu $K\alpha$), K usually taken as 0.89, β the line width at half-maximum height after subtraction of broadening caused by equipment, and θ is the diffraction angle. The XRD profiles of (111) plane of our samples are shown in Fig. 2, which is used to calculate the grain size and lattice parameters. The results are listed in Table 2.

It can be expected that the hydrolysis reaction of tetrabutyl titanate prior to the nanocrystal formation becomes kinetically more efficient in the presence of water [19,20] and consequently leads to an increase in grain size. This provides a very useful means to control the particle size by adding a suitable amount of water to the reaction mixture [21]. In our system, absolute
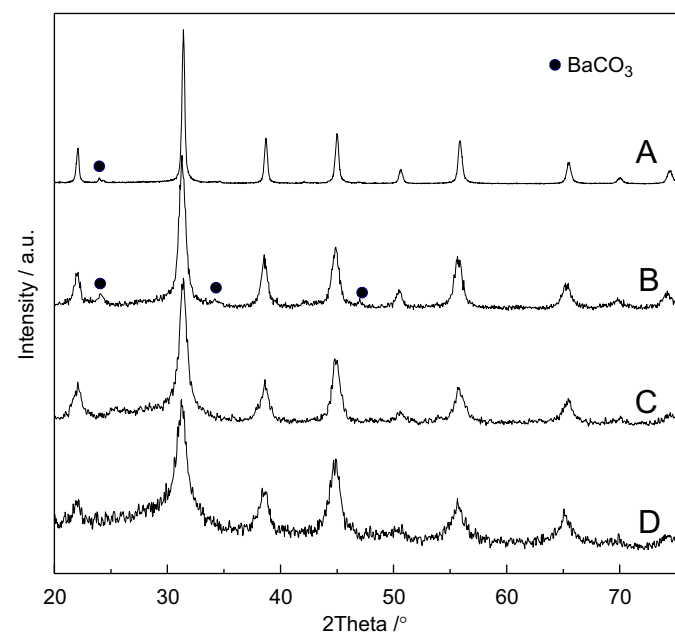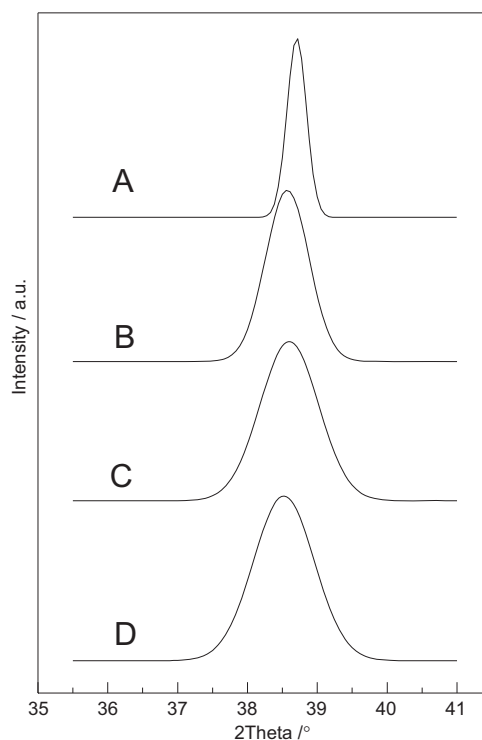

Fig. 1. The XRD profiles of the as-prepared nanoparticles. (A) Ethanol as dispersant and $Ba(OH)_2 \cdot 8H_2O$ + 50.0 g H_2O as raw materials, (B) ethanol as dispersant and $Ba(OH)_2 \cdot 8H_2O$ as raw materials, (C) ethanol as dispersant and $Ba(OH)_2$ + 2H_2O as raw materials, and (D) butanol as dispersant and $Ba(OH)_2$ + 2H_2O as raw materials.

Fig. 2. XRD profile of (111) plane of the as-prepared samples.

ethanol is used as a dispersant during synthesis of samples A, B, and C whereas the water content is different among each systems. In the range of our experiments, the grain size of final $BaTiO_3$ nanoparticles is nearly linear with the molar ratio of water to the

Table 2
Water content and analysis results on XRD profiles.

Samples	Mole ratio of water to Ba during synthesis	Grain size (nm)	Cell constant (Å)
A	35	40	4.0289
B	8	14.6	4.0428
C	2	10.3	4.0399
D	2	6.8	4.0477

Fig. 3. Relationship between grain size of $BaTiO_3$ and water content of system.

Ti (here is the mole number of tetrabutyl titanate) as

$$d = 6.8 + 0.977c \qquad (2)$$

where d is grain size with its unit nm, c is the molar ratio of the mole number of water (include both crystaline water and free water) to that of tetrabutyl titanate. The results are clearly shown in Fig. 3 and Table 2. In sample A, molar ratio of water to Ti ~35 results in the biggest grain size of 40 nm. In sample B, the molar ratio is 8 (here the system has only 8 crystallization water in raw material of $Ba(OH)_2 \cdot 8H_2O$) and the grain size is 14.6 nm. Sample C has the lowest water content as the molar ratio is 2, and grain size is 10.3 nm. The microstructure of the as-synthesized nanoparticles are further characterized by SEM and TEM. A representative SEM images of samples A, B, and C are shown in Fig. 4. It is observed that the particles are uniform, with the grain sizes ~40 nm in sample A, ~15 nm in sample B and ~10 nm in sample C. The results are in good agreement with the XRD estimations. For sample D with a rather smaller grain size, TEM is used for a detailed observation, as shown in Fig. 5. The left of Fig. 5 is a low magnitude image and the average grain size is estimated as ~7 nm, which also agrees well with the XRD estimation. The high magnitude image of sample D is shown on the right of Fig. 5. Regularly arranged patterns can be observed in the darker region of the image, indicating that the particles under observation are well crystallized. Three kinds of lattice patterns are observed, with their spacings 4.05, 2.87 and 2.35 Å, which match the (100), (110) and (111) lattice planes, respectively. The grain size of sample D is smaller than that of sample C. The only difference in the synthesis process between samples C and D is the dispersant, i.e., ethanol is used in sample C and butanol in sample D. This indicates that the grain coarsening rate decreases with increase in the alkanol chain length of the dispersant.

The mechanism of crystal growth is important for the synthesis of a material. Two distinct steps during precipitation of $BaTiO_3$ nanoparticles from aqueous solution are suggested [22]. The first is rapid one to form a titanium hydroxide gel (THG) phase. The second is slower one to form crystalline $BaTiO_3$ through the reaction between the THG phase and the Ba^{2+} ions
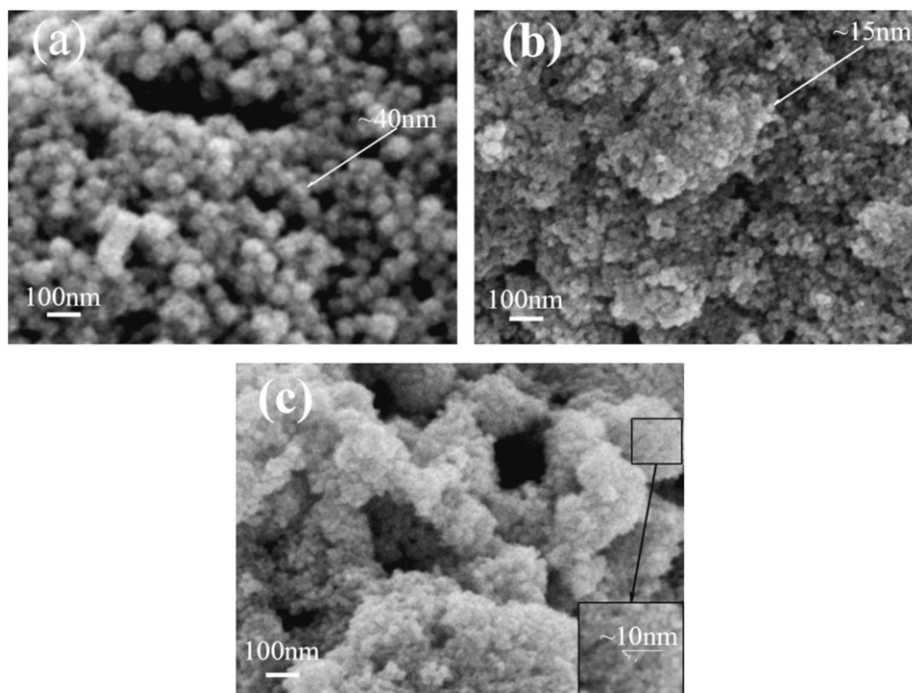

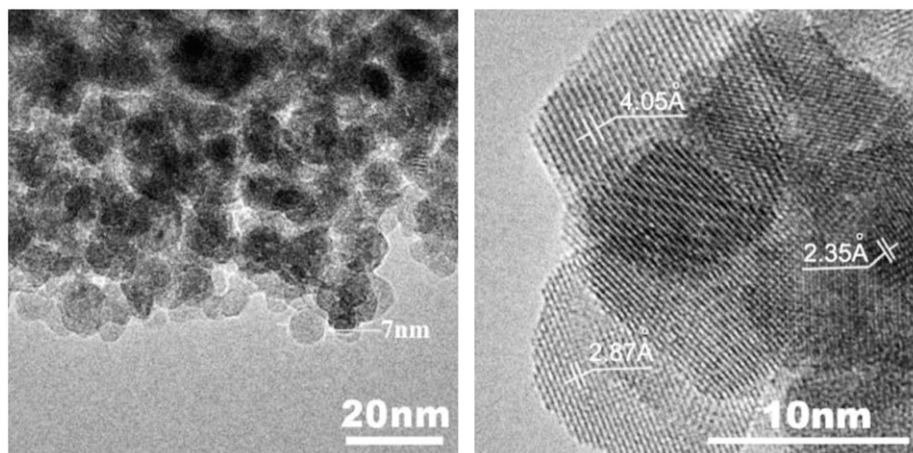**Fig. 4.** SEM images, (a) sample A, (b) sample B, and (c) sample C.
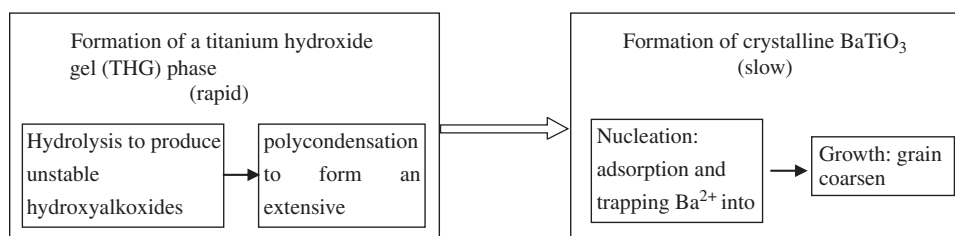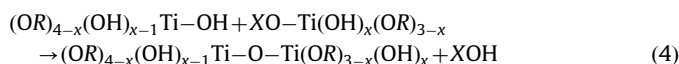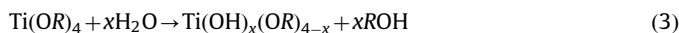
Fig. 5. TEM image of sample D.

**Fig. 6.** Scheme of the mechanism of precipitation of BaTiO$_3$ nanoparticles from solution.

in solution. As a result, the overall kinetics is controlled by the crystallization process.

In the initial step, growth of the Ti–O–Ti network of THG, is known to proceed through another two main stages [23–25], hydrolysis (Eq. (3)) to produce unstable hydroxyalkoxides Ti(OH)$_x$(OR)$_{4-x}$ and polycondensation reactions (Eq. (4)) viaolation or oxolation (i.e., preferential elimination of water or of alcohol, respectively), leading to an extensive Ti–O–Ti network:

$$Ti(OR)_4 + xH_2O \rightarrow Ti(OH)_x(OR)_{4-x} + xROH \qquad (3)$$

$$(OR)_{4-x}(OH)_{x-1}Ti-OH + XO-Ti(OH)_x(OR)_{3-x}$$
$$\rightarrow (OR)_{4-x}(OH)_{x-1}Ti-O-Ti(OR)_{3-x}(OH)_x + XOH \qquad (4)$$

where $R=-CH_2(CH_2)_2CH_3$; $X=H, R$

The entangled networks of THG form polymeric chains during the hydrolysis of Ti salt at a high pH value. The skeleton is composed of –Ti–O–Ti–oxolation and the THG phase formula unit is indicated as TiO(OH)$_2$ [22]. Thus, total hydrolysis can be expressed as

$$Ti(OR)_4 + 3H_2O \rightarrow TiO(OH)_2(gel) + 4ROH \qquad (5)$$
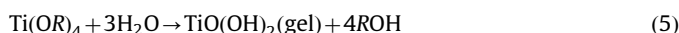
The formation of crystalline BaTiO$_3$ from solution is the slower step. The mechanism is demonstrated as a nucleation and growth [26]. Ba^{2+} ions are expected to be adsorbed at the surface or trapped in the pores of the –Ti–O–Ti–oxolation network [27]. Therefore, the nucleation and growth of the perovskite is represented as

$$TiO(OH)_2(gel) + Ba^{2+}(solution) + 2OH^-(solution)$$
$$\rightarrow BaTiO_3(solid) + 2H_2O(solution) \qquad (6)$$
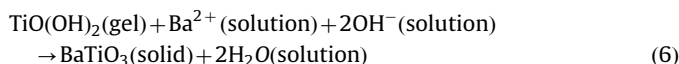
Generally, the hydrolysis and formation of THG are very fast and proceed at once in the presence of a quantity of water [20]. However, if there is not much water in the reaction system, the formation of THG has to be ceased. Therefore, when the water content is controlled to a small value, all the precipitation should

be dominated by the water balance, i.e. the rapid step needs water as shown in Eq. (5) and slower step produces water as shown in Eq. (6), thus controls the crystallization of BaTiO$_3$ nanoparticles. During the crystallization of BaTiO$_3$ nanoparticles from solution, the concentration of the reaction ions such as Ba^{2+} and OH$^-$ as shown in Eq. (6) is also important. A larger content of water in the dispersant will lead to a higher solubility of Ba(OH)$_2$ and provides higher concentration of the reaction ions. Under this condition, as the added water content is increased, the rate of crystallization is enhanced and the grain size is increased. In our experiments, during the synthesis of samples A, B, and C, the water content decreases compliably and the grain size of them decreases. To reveal the mechanism of formation of BaTiO$_3$ nanoparticles clearly, the scheme is shown in Fig. 6. There are two steps and two stages separated in each step. Water content is associated with every stage. Therefore, water content in the reaction system offers an efficient method to modulate the grain size of the final products.

Several factors, such as the surface energy, the viscosity, etc. are associated with the grain coarsening rate as [28,29]:

$$k = \frac{8\gamma V_m^2 c_{r=\infty}}{54\pi\eta a N_a} \qquad (7)$$

where k is the growth rate of grain volume, γ the surface energy, V_m the molar volume, and $c_{r=\infty}$ is the equilibrium concentration at a flat surface (i.e., the bulk solubility). η is the viscosity of the solvent, a the solvated ion radius and N_a is the Avogadro constant. The representative value of γ is estimated to be $\sim$0.22 J m^{-2} on the basis of the Gibbs adsorption isotherm [30] and $\sim$0.15 Jm^{-2} from an empirical relationship that correlates the surface tension of oxides with their solubility in water [31], although it can change with different solvents or dispersants. The molar volume for BaTiO$_3$ is 38.5 cm^3 mol^{-1} and is essentially constant. The bulk solubility of BaTiO$_3$ $c_{r=\infty}$ is expected to be related to the lattice enthalpy and the ion solvation enthalpy. For alkanols, η increases with the

increase in chain length, and then the grain coarsening rate decreases. The solvated ion radius a implies a high coordination number of the solvent molecules. As an example, 1-hexanol is about twice as long as an ethanol molecule, the solvated ion radius for barium ions in hexanol would be expected to be about twice the solvated ion radius in ethanol, assuming similar coordination numbers. Thus, the chain length of solvent or dispersant increases, the solvated ion radius increases and the grain coarsening rate decreases. As mentioned and analyzed above, the coarsening rate of $BaTiO_3$ from solution depends on the solvent or dispersant. For the alkanol, the chain length increases, the coarsening rate decreases and the grain size decreases. Therefore, in our experiments, sample D has smaller grain size than sample C.

4. Conclusion

A size-modulable and large-scale synthesis route is developed to obtain perovskite-structured nanoparticles. With this method, $BaTiO_3$ nanoparticles can be synthesized at room temperature directly. The synthesis efficiency is improved greatly and the batch processing can be scaled up easily because large quantity of solvents is not necessary in this method. Their grain size can be modulated by water content and the alkanol chain length of the dispersant efficiently. Less water content and longer alkanol chain length of the dispersant in the synthesis system result in a finer grain size of the nanoparticles. Different nanoparticles with their sizes varying from 7 to 40 nm can be obtained using different water contents and choosing different dispersants. It is noted that both the content of water and the alkanol chain length of the dispersant are dominant in the grain coarsening during the synthesis of the $BaTiO_3$ nanoparticles.

Acknowledgment

References

[1] A. Rae, M. Chu, V. Ganine, Barium titanate—Past, present and future. In Dielectric Ceramic Materials, in: K.M. Nair, A.S. Bhalla (Eds.), Ceramic Transactions Vol. 100; The American Ceramic Society, Westerville, OH, 1999, p. 1–12.
[2] T.G. Reynolds, Am. Ceram. Soc. Bull. 80 (2001) 29.
[3] J.Q. Qi, W.P. Chen, Y.J. Wu, L.T. Li, J. Am. Ceram. Soc. 81 (1998) 437.
[4] S. Wada, T. Tsurumi, H. Chikamori, T. Noma, T. Suzuki, J. Cryst. Growth 229 (2001) 433.
[5] C.W. Beier, M.A. Cuevas, R.L. Brutchey, J. Mater. Chem. 20 (2010) 5074.
[6] J.J. Urban, W.S. Yun, Q. Gu, H.K. Park, J. Am. Chem. Soc. 124 (2002) 1186.
[7] S. O'Brien, L. Brus, C.B. Murray, J. Am. Chem. Soc. 123 (2001) 12085.
[8] M. Niederberger, N. Pinna, J. Polleux, M.R. Antonietti, Angew. Chem. Int. Ed. 43 (2004) 2270.
[9] L.A. Pérez-Maqueda, M.J. Diañez, F.J. Gotor, M.J. Sayagués, C. Real, J.M. Criado, J. Mater. Chem. 13 (2003) 2234.
[10] J.Q. Qi, L.T. Li, Y.L. Wang, Z.L. Gui, J. Cryst. Growth 260 (2004) 551.
[11] D. Feng, K. Kazumi, I. Hiroaki, W. Satoshi, H. Hajime, K. Makoto, Chem. Eng. J. 170 (2011) 333.
[12] J.Q. Qi, Y. Wang, W.P. Chen, L.T. Li, H.L.W. Chan, J. Nanopart. Res. 8 (2006) 959.
[13] N. Nuraje, K. Su, A. Haboosheh, J. Samson, E.P. Manning, N.I. Yang, H. Matsui, Adv. Mater. 18 (2006) 807.
[14] V. Bansal, P. Poddar, A. Ahmad, M. Sastry, J. Am. Chem. Soc. 128 (2006) 11958.
[15] X. Wei, G. Xu, Z.H. Ren, G. Shen, G.R. Han, J. Am. Ceram. Soc. 91 (2008) 3774.
[16] O.E. Teyeb, L. Matthew, K.R. Lyle, N. Krisztian, D. Michael, E.M. Daniel, Nat. Protocols 6 (2011) 97.
[17] J.Q. Qi, L. Sun, Z.W. Ma, T. Peng, B.B. Liu, L.T. Li, CN 201010129715.9.
[18] J.Q. Qi, L. Sun, Y. Wang, W.P. Chen, P. Du, Y.G. Xu, L.T. Li, C.W. Nan, H.L.W. Chan, Adv. Powder Tech. 22 (2011) 401.
[19] S. Yoon, S. Baik, M.G. Kim, N. Shin, I. Kim, J. Am. Ceram. Soc. 90 (2007) 311.
[20] P.D. Cozzoli, A. Kornowski, H. Weller, J. Am. Chem. Soc. 125 (2003) 14539.
[21] Y.V. Kolen'ko, K.A. Kovnir, I.S. Neira, T. Taniguchi, T. Ishigaki, T. Watanabe, N. Sakamoto, M. Yoshimura, J. Phys. Chem. C 111 (2007) 7306.
[22] A. Testino, V. Buscaglia, M.T. Buscaglia, M. Viviani, P. Nanni, Chem. Mater. 17 (2005) 5346.
[23] B.L. Bischoff, M.A. Anderson, Chem. Mater. 7 (1995) 1772.
[24] T. Sugimoto, X. Zhou, A. Muramatsu, J. Colloid Interface Sci. 259 (2003) 43.
[25] Q. Zhang, L. Gao, Langmuir 19 (2003) 967.
[26] A. Testino, M.T. Buscaglia, V. Buscaglia, M. Viviani, C. Bottino, P. Nanni, Chem. Mater. 16 (2004) 1536.
[27] D. Hennings, G. Rosenstein, H. Schreinemacher, J. Eur. Ceram. Soc. 8 (1991) 107.
[28] E.M. Wong, J.E. Bonevich, P.C. Searson, J. Phys. Chem. B 102 (1998) 7770.
[29] Z. Hu, G. Oskam, P.C. Searson, J. Colloid Interface Sci. 263 (2003) 454.
[30] A. Mersmann, J. Cryst. Growth 102 (1990) 841.
[31] O. Sonhel, J. Garside, Precipitation: Basic Principles and Industrial Applications, Butterworth & Heinemann, , 1992, pp 37–39.